Identification of highly active iron sites in N_2O-activated Fe/MFI

Jifei Jia [a], Qi Sun [a], Bin Wen [a], Lin X. Chen [b], and Wolfgang M.H. Sachtler [a,*]

[a] *Institute for Environmental Catalysis, Northwestern University, Evanston, IL 60208, USA*
[b] *Chemistry Division, Argonne National Laboratory, Argonne, Illinois 60439, USA*

Received 8 February 2002; accepted 29 March 2002

Reduction in an H_2 flow at 600 °C of Fe/MFI prepared by chemical vapor deposition, followed by its exposure to N_2O at 250 °C, produces a highly active state characterized by an unusual TPR spike at 200 °C. *In situ* X-ray absorption near-edge structure, X-ray absorption fine structure data and literature data on DFT calculations suggest that in this state some Fe will be present in the oxidation state of Fe^{4+}.

KEY WORDS: oxidation state >3 of Fe; Fe in MFI; α-sites; N_2O dissociation; *in situ*; XANES; XAFS.

1. Introduction

Fe/MFI catalysts (the zeolite MFI is often called ZSM-5) and their interaction with nitrogen oxides have recently attracted much attention. Panov *et al.* [1,2] showed that Fe/MFI catalysts with low iron loading catalyze the oxidation of benzene with nitrous oxide to phenol in one step. Over high Fe loaded catalysts, especially those prepared by chemical vapor decomposition of $FeCl_3$ on H-MFI, the nitrogen oxides NO and NO_2 are efficiently reduced to N_2 with hydrocarbons [3,4] or ammonia [5]. For these materials the formation of oxygen-bridged Fe dimers was confirmed by the X-ray absorption fine structure (XAFS) data of Marturano *et al.* [6] and Battiston *et al.* [7]. Over such Fe/MFI catalysts N_2O decomposition was found to display kinetic oscillation in the presence of water vapor [8]. Disproportionation of NO to $N_2O + NO_2$ was also observed over some catalysts of this class [9,10].

Panov *et al.* [1,2] observed that Fe/MFI catalysts with low Fe loading that were treated at a high temperature are able to abstract an oxygen atom from an impinging N_2O molecule at 250 °C, without releasing O_2 to the gas phase. These authors call this special form of adsorbed oxygen "α oxygen". Its nature is subject to much debate.

Yoshizawa *et al.* [11] assumed that an $[FeO]^+$ adduct is formed which is reduced, in a catalytic cycle, to Fe^+. Yakovlev *et al.* recently [12] published an extensive DFT analysis of the interaction of N_2O with an Fe/MFI catalyst having the majority of Fe ions as oxygen-bridged dimer ions, $[HO{-}Fe{-}O{-}Fe{-}OH]^{2+}$, with Fe^{3+}. At high temperature and upon reduction they are transformed to $[Fe{-}O{-}Fe]^{2+}$ ions with Fe^{2+}. These authors conclude that interaction of N_2O with the latter ion transforms it into an $[Fe{-}O{-}Fe{-}O]^{2+}$ ion with a terminal $Fe^{4+}{-}O^-$ bond, while N_2 is released. For the terminal Fe–O group their calculations predict an Fe–O distance of 1.61 Å, indicating double bond character, although the spin density at the O atom is near unity. For the exothermic process:

$$[Fe{-}O{-}Fe]^{2+} + N_2O = [Fe{-}O{-}Fe{-}O]^{2+} + N_2 \quad (1)$$

a standard reaction enthalpy of $\Delta H_1 = -132$ kJ/mol is calculated. From this value it follows that subsequent reduction with H_2:

$$[Fe{-}O{-}Fe{-}O]^{2+} + H_2 = [Fe{-}O{-}Fe]^{2+} + H_2O \quad (2)$$

should be exothermic by 192 kJ/mol. Much lower values are calculated for the interaction of N_2O with hydrated Fe dimers. Arbuznikov and Zhidomirov [13] did *ab initio* calculations and found values of 50 or 240 kJ/mol, depending on the assumed structure, for the interaction of N_2O with twofold-bridged and hydroxylated Fe dimers in MFI.

In previous papers we reported ESR results showing the formation of superoxide ions, O_2^-, upon exposing Fe/MFI to O_2 at −196 °C [14], and Raman data indicating that peroxide ions, O_2^{2-}, were formed at 25 °C [15]. In the present paper we report on experimental results of the interaction of N_2O with dehydrated and partially reduced Fe/MFI having a molar ratio of Fe to Al-centered tetrahedra of 1/1. We have characterized this material by H_2-TPR and *in situ* XANES and XAFS.

2. Experimental

2.1. Preparation of Fe/MFI

H/MFI was obtained by three-fold ion exchange Na/MFI (Si/Al = 23, UOP) with a diluted NH_4NO_3 solution at ambient temperature, followed by calcination of the NH_4^+ form of the zeolite in a UHP O_2 flow at 550 °C

* To whom correspondence should be addressed, at V. N. Ipatieff Laboratory, Center for Catalysis and Surface Science, Northwestern University, 2137 Sheridan Road, Evanston, IL 60208, USA.
E-mail: wmhs@northwestern.edu

1011-372X/02/0900-0007

for 4 h. Sublimation of $FeCl_3$ in an Ar flow at 320 °C was used by directing the vapor onto the heated H/MFI. The detailed procedure was described in our previous paper [4]. After hydrolysis, the slurry was vacuum filtered and the solid was washed throughly with DDI water, dried at 120 °C in air and calcined in O_2 at 500 °C. The Fe/Al ratio is near unity, which corresponds to 4.0 wt% Fe for the dry catalyst.

2.2. Temperature-programmed reduction (TPR)

H_2-TPR experiments were performed with an H_2/Ar (5%) flow of 40 ml/min from 25 to 600 °C with a ramp of 8 °C/min. The H_2 consumption was determined by a TCD detector, with H_2O being trapped in a dry-ice cooled trap. CuO/SiO_2 (quartz) was used as a standard to calibrate the consumption of H_2.

2.3. N_2O treatment

Treatment of Fe/MFI with N_2O was performed at 250 °C in a recirculating manifold equipped with a Dycor quadrupole gas analyzer. 0.2 g Fe/MFI was charged in a U-shaped Pyrex reactor having a bypass valve. The volume of the circulation loop is 145 ml when the reactor is bypassed, but 166 ml when the reactor is open. An electromagnetic-driven gas circulation pump was installed inside the loop to thoroughly mix the gas and enforce its circulation through the catalyst bed with a flow rate of 100 ml/min. A mixture of 30 Torr N_2O, 20 Torr Ar and 70 Torr He was used. All mass spectrometric signal intensities were normalized with respect to the Ar^{2+} peak ($m/e = 20$).

2.4. In situ X-ray absorption fine structure (XAFS)

In situ XANES/XAFS measurements were performed at Beamline 12BM of the Advanced Photon Source (APS) at Argonne National Laboratory, USA, with an Si(111) crystal in the monochromator. Each sample was loaded in a reactor constructed for *in situ* XAFS measurements, where two Mylar windows before and after the sample allowed the transmission measurements and were well-insulated from the heater surrounding the sample. The Fe *K*-edge spectra were collected in the transmission mode at room temperature. For the *in situ* treatment with N_2O the sample was exposed to flowing N_2O of 1 bar. Data analysis was carried out using WinXAS provided by T. Ressler, Hamburg, Germany. Reference spectra were calculated using the FEFF8.10 program [16]. The Fourier transform (FT) of the k^3-weighted XAFS spectra was carried out within $k = 3$–$13\,\text{Å}^{-1}$. The structural parameters were extracted from the back Fourier transform of each peak or the first two peaks in the FT-XAFS spectrum with a 2% Hanning window. Each peak was first fit to a single neighboring shell. Subsequent fits with more neighboring shells were carried out until the result was satisfactory. In order to minimize the artifacts from introducing additional parameters, we only present the two-shell model when the residuals of the fit were approximately one-half of those from a single-shell fit.

3. Results and discussion

Figure 1 shows H_2-TPR profiles of Fe/MFI after a variety of treatments. Profile (a) was found after

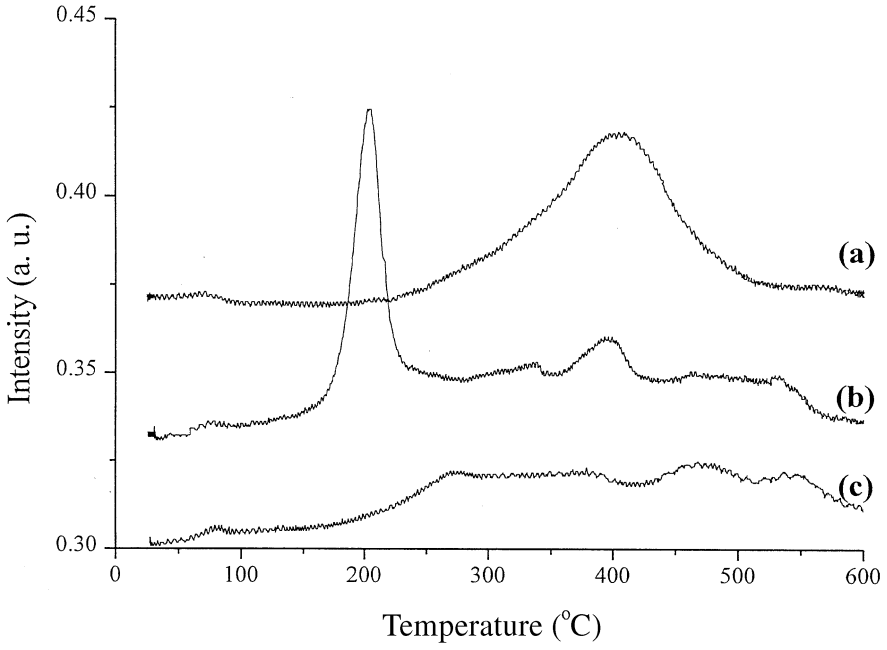

Figure 1. H_2-TPR of Fe/MFI. (a) After calcination in O_2 at 500 °C, (b) after reduction in H_2 at 600 °C, followed by exposure to N_2O at 250 °C, and (c) after reduction in H_2 at 600 °C, followed by exposure to O_2 at 250 °C.

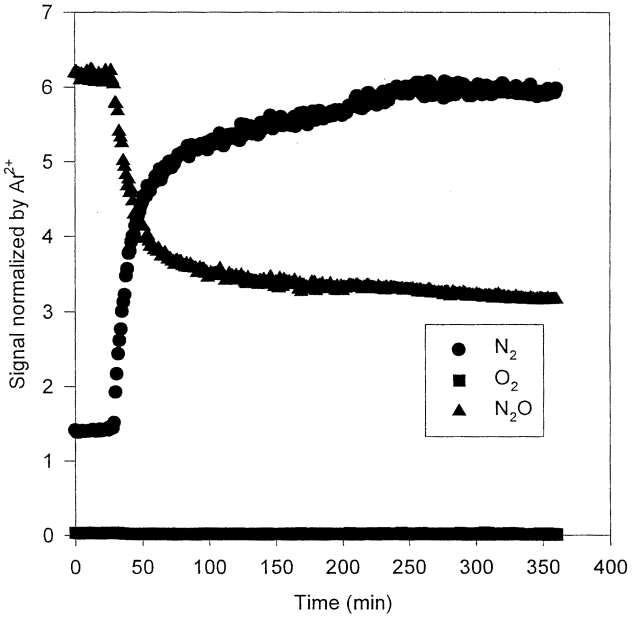

Figure 2. N_2O dissociative adsorption at 250 °C on Fe/MFI which was prereduced at 600 °C by H_2.

calcination in flowing O_2 at 500 °C. A broad peak at 410 °C is observed. After recording this H_2-TPR up to 600 °C, the Fe/MFI was exposed to N_2O at 250 °C. Figure 2 shows that N_2O ($m/e = 44$) is dissociatively chemisorbed and N_2 is released. This reaction appeared to be completed in about 250 min. As no gas-phase O_2 was produced, the number of O atoms deposited at the surface is equal to the number of N_2 molecules detected in the gas. In this state, the oxidized Fe/MFI was subjected to H_2-TPR, and the result is shown in profile (b) of figure 1. A sharp spike at 200 °C is most prominent. The high exothermicity of this reduction event was apparent from the marked deviation of the temperature from the programmed value. Clearly, the chemical signature of this Fe–oxygen complex is different from that of the bridging oxygen, the superoxide ion and the peroxide ion detected in our previous work on Fe/MFI exposed to O_2. It is, however, consistent with the chemistry predicted for reaction (2). Profile (b) also shows some broad peaks of low intensity between 280 and 600 °C. Profile (b) is similar to recent TPR results reported by Mauvezin *et al.* [17]. After the TPR run (a), the sample was also exposed to O_2 and another TPR profile was measured, shown as trace (c) in figure 1. No spike is visible at 200 °C; this signal is thus specific for the material activated by N_2O.

In situ XANES and XAFS measurements were done to identify the species responsible for the unique TPR peak at 200 °C. XANES spectra of Fe/MFI registered at room temperature are shown in figure 3 in three states: (a) after calcination in O_2 at 500 °C, (b) after subsequent reduction in H_2 at 600 °C, and (c) after exposing the material of (b) to N_2O at 250 °C. Clearly, the Fe *K*-edge shift demonstrates both the reduction and the reoxidation processes. The Fe in sample (a) can be best described as Fe^{3+}, because its *K*-edge position matches well with that of α-Fe_2O_3 (not shown). Reduction of Fe^{3+} by heating in H_2 from room temperature to 600 °C was monitored *in situ* by XANES (not shown). A shift of the Fe *K*-edge to lower energy clearly indicates reduction of Fe^{3+} to Fe^{2+} and Fe(0). Reoxidation by N_2O is confirmed by the shift of the Fe *K*-edge back to higher energy.

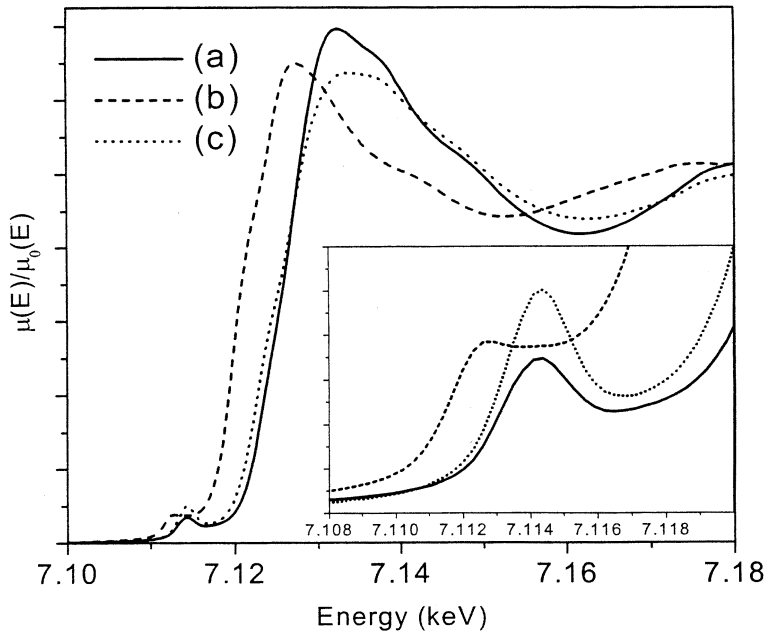

Figure 3. *In situ* Fe *K*-edge XANES spectra of Fe/MFI. (a) Calcined by O_2 at 500 °C, (b) reduced by H_2 at 600 °C, and (c) reduced at 600 °C by H_2, followed by exposure to N_2O at 250 °C.

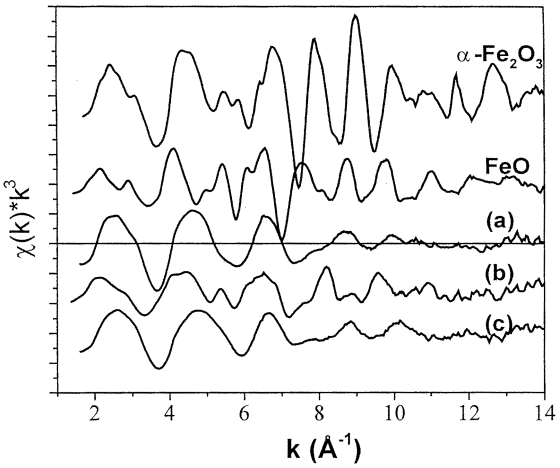

Figure 4. k^3-Weighted XAFS spectra of α-Fe_2O_3, FeO and Fe/MFI calcined in flowing O_2 at 500 °C (a), reduced by H_2 at 600 °C (b), and reduced at 600 °C by H_2 and then exposed to N_2O at 250 °C (c).

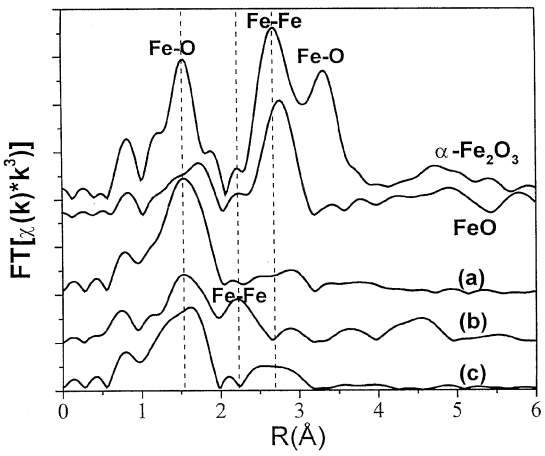

Figure 5. Fourier-transformed XAFS spectra for the same samples as in figure 4.

Most remarkably, the pre-edge peak intensity in the XANES spectrum of sample (c) is about 50% higher than that of sample (a) (figure 3 inset). Pre-edge peaks of the *K*-edge are normally very weak in a centrosymmetric coordination environment, because they originate from the dipole-forbidden 1*s* to 3*d* transitions [18]. Their intensities are enhanced when the coordination symmetry of the metal deviates severely from a centrosymmetric environment, as this enhances the dipole-allowed 1*s* to 4*p* transitions due to mixing of 3*d* and 4*p* orbitals of the transition metal atom. The amount of the 4*p* component mixed with 3*d* orbitals as a function of the metal coordination geometry has been shown to vary from 0 for an octahedral coordination to 7.5% for a tetrahedral coordination [19]. Thus, the higher pre-edge peak intensity in sample (c) suggests an average coordination geometry that is less centrosymmetric compared to that in sample (a). Fe ions in an oxidation state >3 have a smaller radius than Fe in a lower oxidation state and are, therefore, more likely to adopt a tetrahedral coordination with oxygen ions [20]. If the higher pre-edge peak intensity of Fe in sample (c) is indeed due to the presence of tetrahedral Fe sites, it follows that this Fe is likely in an oxidation state higher than Fe^{3+}. This tentative conclusion is subjected to further proof by XAFS data analysis.

Figure 4 shows XAFS spectra of the same three samples as in figure 3, along with those for α-Fe_2O_3 and FeO as references. The spectrum for sample (a) is very similar to α-Fe_2O_3 in the low *k* region, but it deviates significantly in the high *k* region and lacks certain fine features that are present in the α-Fe_2O_3 spectrum. Similarly, the spectrum for sample (b) resembles that of FeO in the low *k* region. Although the general features in the spectra of sample (a) and (c) are similar, there are observable differences between the two. The FT-XAFS spectra for the same three samples shown in figure 5 clearly demonstrate that.

Figure 5 also shows that sample (a) has a nearest-neighbor peak corresponding to an Fe−O distance similar to that in α-Fe_2O_3, although the peak is broader, indicating a wider distance distribution. However, the distant Fe−Fe and Fe−O peaks at about 2.7 and 3.3 Å (without phase correction) in α-Fe_2O_3 are essentially absent in sample (a). This suggests that: (1) the Fe ions in this sample are highly dispersed and (2) the material is severely disordered. Sample (b) has an intense second peak at about 2.2 Å (without phase correction), corresponding to the Fe−Fe distance in metallic iron. Therefore, this sample contains both Fe^{2+} and Fe(0). Apparently, the XANES edge-shift is due to both Fe^{2+} and Fe(0). The nearest-neighbor Fe−O peak in the spectrum of sample (c) displays a shoulder at a shorter distance, which suggests the existence of a distinctively different Fe−O distance compared to sample (a).

The results from data analysis are given in table 1. For sample (a), the Fe−Fe distance is 3.02 Å and the coordination number is 1.1. This indicates that the Fe is in an oxygen-bridged dinuclear entity, in agreement with the XAFS data of Marturano *et al.* [6]. As mentioned earlier, fitting results for the spectrum of

Table 1
XAFS-derived coordination numbers (CN), shell radius (R) and Debye–Waller factor (σ^2) of Fe/MFI after different treatments

Treatment	Shell	CN	R (Å)	σ^2 (Å^2)
Calcined by O_2 at 500 °C	Fe−O	1.7 ± 0.3	1.93 ± 0.02	0.006
	Fe−O	3.4 ± 0.5	2.09 ± 0.02	0.008
	Fe−Fe	1.1 ± 0.3	3.02 ± 0.02	0.02
Reduced by H_2 at 600 °C	Fe−O	0.9 ± 0.4	2.23 ± 0.02	0.003
	Fe−O	2.3 ± 0.5	2.06 ± 0.02	0.007
	Fe−Fe	0.8 ± 0.4	2.47 ± 0.02	0.007
Reduced by H_2 at 600 °C	Fe−O	0.4 ± 0.2	1.81 ± 0.02	0.002
and then activated by N_2O	Fe−O	3.5 ± 0.5	2.03 ± 0.02	0.01
at 250 °C	Fe−Fe	2.6 ± 0.5	3.00 ± 0.02	0.01

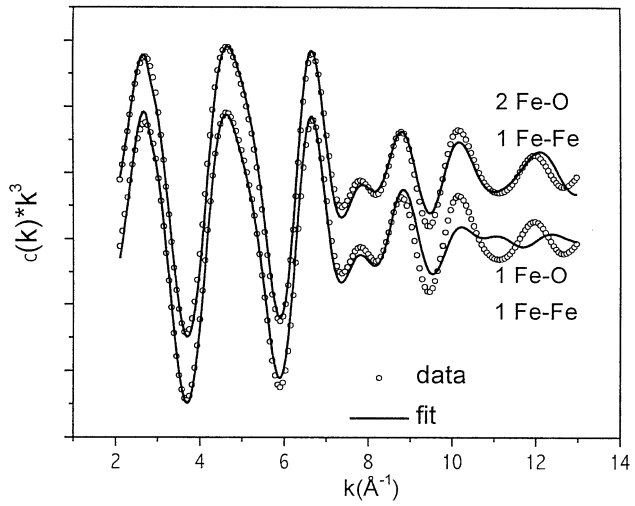

Figure 6. Data-fitting results for reoxidized Fe/MFI in N_2O at 250 °C with one and two Fe–O distances for the nearest neighbors. The residuals are 19.7 and 11.2 for the fits, respectively.

sample (c) favor two Fe-O distances in the nearest neighboring shell. The longer Fe–O distance of 2.03 Å is attributed to the majority Fe^{3+} species, whereas the shorter Fe–O distance of 1.81 Å is due to a minority Fe species of a higher oxidation state. Figure 6 shows that only fitting with two Fe–O values is matching the data. Most remarkably, the minority species with a shorter Fe–O distance was observed only in sample (c). It thus supports that the material which is responsible for the TPR spike at 200 °C is unique in having small Fe ions with a shorter Fe–O distance than found with Fe^{3+}. The Fe–O distance of 1.81 Å is longer than the value of 1.61 Å predicted by Yakovlev *et al.* [12] for the terminal Fe^{4+}–O^{-} group with strong double bond character. It agrees, however, with the value for Fe^{4+}–O reported by Kemner *et al.* [21], who compared ferrates with different oxidation states of Fe and found a linear relationship between iron oxidation state and Fe–O distance.

The following picture appears to emerge: coordinatedly unsaturated Fe^{2+} ions are formed during reduction at 600 °C. They react with N_2O to form an Fe–oxygen complex that is distinctly different from the material obtained by exposure to O_2. For the new ferryl groups, the present data suggest that Fe is in the oxidation state of Fe^{4+}. A tentative assignment of the TPR peaks in figure 1(b) appears possible: the TPR spike at 200 °C is related to the reduction of the ferryl group with the Fe–O distance of 1.81 Å, whereas the weaker broad TPR peaks between 280 and 600 °C are related to the reduction of Fe with an Fe–O distance of 2.03 Å. In Panov's Fe/MFI catalyst with an iron content of 0.53 wt%, the concentration of "α oxygen" is 1.8×10^{19} sites/g corresponding to a molar ratio $O_\alpha/Fe = 0.3$ [1]. For the present Fe/MFI with 4.0 wt% Fe, integration of the TPR spike at 200 °C results in 1.1×10^{20} sites/g, or $O_{200}/Fe = 0.25$. It thus seems probable that in both cases the oxygen atoms are bonded to Fe^{4+} ions.

4. Acknowledgments

This work was supported by the EMSI program of the National Science Foundation and the U.S. Department of Energy, Office of Science (CHE-9810378) at the Northwestern University Institute for Environmental Catalysis (IEC). Support from the Director of the Chemistry Division, BES, U.S. Department of Energy, Grant DE-FGO2-87ER13654, is gratefully acknowledged. IEC work at Argonne National Laboratory is supported by the U.S. Department of Energy, Office of Basic Energy Sciences, Division of Chemical Sciences, under contract W-31-109-Eng-38. The authors thank Dr. Tao Liu for his help in data collection and Dr. Jennifer Linton for her assistance in beam line operation at the BESSRC-CAT, Advanced Photon Source.

References

[1] G.I. Panov, A.K. Uriarte, M.A. Rodkin and V.I. Sobolev, Catal. Today 41 (1998) 365.
[2] G.I. Panov, CatTech 7 (2000) 18.
[3] W.K. Hall, X. Feng, J. Dumesic and R. Watwe, Catal. Lett. 52 (1998) 13.
[4] H.Y. Chen and W.M.H. Sachtler, Catal. Today 42 (1998) 73.
[5] Q. Sun, Z. Gao, H.Y. Chen and W.M.H. Sachtler, J. Catal. 201 (2001) 89.
[6] P. Marturano, L. Drozdová, A. Kogelbauer and R. Prins, J. Catal. 192 (2000) 236.
[7] A.A. Battiston, J.H. Bitter and D.C. Koningsberger, Catal. Lett. 66 (2000) 75.
[8] El M. El Malki, R.A. van Santen and W.M.H. Sachtler, Microporous and Mesoporous Materials 35 (2000) 235.
[9] G.D. Lei, B.J.Adelman, J Sárkány and W.M.H. Sachtler; Appl. Catal. B 112 (1995) 245.
[10] T. Beutel, J. Sárkány, J.Y. Yan and W.M.H. Sachtler; J. Phys. Chem. 100(2) (1996) 845.
[11] K. Yoshizawa, T. Yumura, Y. Shiota and T. Yamabe, Bull. Chem. Soc. Japan 73 (2000) 29.
[12] A.L. Yakovlev, G.M. Zhidomirov and R.A. van Santen, J. Phys. Chem. B 105 (2001) 12297.
[13] A.V. Arbuznikov and G.M. Zhidomirov, Catal. Lett. 40 (1996) 17.
[14] E. El-Malki, D. Werst, P.E. Doan and W.M.H. Sachtler, J. Phys. Chem. B 104 (2000) 5924.
[15] Z. Gao, H. Kim, Q. Sun, P. Stair and W.M.H. Sachtler, J. Phys. Chem. B 105 (2001) 6186.
[16] J.L. Mustre; J.J.Rehr and S.I. Zabinsky, Phys. Rev. B 44 (1991) 4146.
[17] M. Mauvezin, G. Delahay, B. Coq, S. Kieger, J.C. Jumas and J. Olivier-Fourcade, J. Phys. Chem. B 105 (2001) 928.
[18] D.C. Koningsberger and R. Prins (Eds.) *X-ray Absorption: Principles, Applications, Techniques of EXAFS, SEXAFS and XANES* (Wiley, 1988), *Chemical Analysis* Vol. 92, p. 87.
[19] T.E. Westre, P. Kennepohl, J.G. DeWitt, B. Hedman, K.O. Hodgson and E.I. Solomon, J. Am. Chem. Soc. 119 (1997) 6297.
[20] W. Klemm, C. Brendel and G. Wehrmeyer, Chem. Ber. 98 (1960) 1505.
[21] K.M. Kemner, S.D. Kelly, K.A. Orlandini, A.I. Tsapin, M.G. Goldfeld, Y.D. Perfilliev and K.H. Nealson, J. Synchrotron Rad. 8 (2001) 949.